

# Relativistic dips in entangling power of gravity

Marko Toroš<sup>1</sup>, Martine Schut<sup>2</sup>, Patrick Andriolo<sup>3</sup>, Sougato Bose<sup>4</sup>, and Anupam Mazumdar<sup>2</sup>

<sup>1</sup>*Faculty of Mathematics and Physics, University of Ljubljana, Jadranska 19, SI-1000 Ljubljana, Slovenia*

<sup>2</sup>*Van Swinderen Institute, University of Groningen, Groningen 9747 AG, The Netherlands*

<sup>3</sup>*Physics Institute, University of São Paulo, Rua do Matão, 1371, São Paulo, Brazil*

<sup>4</sup>*University College London, Gower Street, WC1E 6BT London, United Kingdom*



(Received 20 June 2024; accepted 21 January 2025; published 21 February 2025)

The salient feature of both classical and quantum gravity is its universal and attractive character. However, less is known about the behavior and build-up of quantum correlations when quantum systems interact via graviton exchange. In this work, we show that quantum correlations can remain strongly suppressed for certain choices of parameters even when considering two adjacent quantum systems in delocalized states. Using the framework of linearized quantum gravity with post-Newtonian contributions, we find that there are special values of delocalization where gravitationally induced entanglement drops to negligible values, albeit nonvanishing. We find a pronounced cancellation point far from the Planck scale, where the system tends toward classicalization. In addition, we show that quantum correlations begin to reemerge for large and tiny delocalizations due to Heisenberg's uncertainty principle and the universal coupling of gravity to the energy-momentum tensor, forming a valley of gravitational entanglement.

DOI: [10.1103/PhysRevD.111.036026](https://doi.org/10.1103/PhysRevD.111.036026)

## I. INTRODUCTION

The coupling of classical gravity to the stress-energy tensor has been probed in numerous experiments and has withstood the test of time in all astronomical observations [1]. One of its most distinguishing consequences is the universal and attractive character of the induced gravitational matter-matter interaction. Such behavior is manifest by looking at Newton's  $1/r$  potential, but persists also when including post-Newtonian (PN) corrections depending on the particle momenta [2–6].

The same universal and attractive behavior is also a feature of an effective field theory of quantum gravity [4], where the gravitational field is not real-valued but rather operator-valued [7–10]. Such a quantum interaction can generate nonclassical correlations between quantum systems with no classical analogue, making it ideal for testing genuinely quantum aspects. This observation was critical in conceiving a protocol to test the quantum nature of gravity using two massive particles [11,12].<sup>1</sup> This protocol, known as the quantum gravity-induced entanglement of masses (QGEM), is in this regard akin to Bell's original idea of

testing quantum correlations between two spatially separated systems [14,15].

According to the local operations and classical communication (LOCC) principle [16], entanglement can only be generated by ostensibly quantum interactions between the test particles. Hence, only if gravity is a quantum entity will it generate an entangled state of the two masses [11,17]. Within the context of an effective field theory of quantum gravity the gravitational interaction is being mediated by the massless spin-2 graviton, see [4,7–10,17–24], for a textbook, see [25].

Theoretical works and feasibility studies about the QGEM proposal have mainly focused on the static regime where the momenta of the particles (i.e., the PN corrections) are neglected in the gravitational interaction. In the static Newtonian limit, the interaction is in position, and the spatial delocalizations of the quantum states control entanglement generation. Generally speaking, increasing the spatial delocalization  $\Delta x$  will increase the overall generated entanglement. Based on the intuition from the static Newtonian limit, decreasing the spatial delocalization  $\Delta x$  would suggest that the generated entanglement is bound to decrease. We will show that this is not the case and that this naive picture breaks down when the PN corrections are included in the analysis [26].

In this paper, we will show that the generated entanglement in general increases for both very small and very large spatial delocalizations  $\Delta x$ . This observation is, in a way, simple, and it follows directly from Heisenberg's uncertainty principle [27] and the universal coupling of gravity to energy [28]. The generated entanglement entropy, quantifying the degree of entanglement, scales as a function of  $\Delta x$

<sup>1</sup>The results of Ref. [11] were already known earlier, see [13].

for large spatial delocalizations and as a function of  $\Delta p \propto \hbar/\Delta x$  for small spatial delocalizations. We will illustrate this result using a toy setup of two harmonic oscillators interacting gravitationally for the initial state of the product of ground states.

There is also an unexpected twist in the story. We find small pockets in the parameter space of  $\Delta x$ —far from the Planck scale—where the entanglement is strongly suppressed. This decrease is pronounced when the dominant 0PN and 1PN terms entering in the generation of quantum correlations cancel each other's contributions. The explanation lies in the opposite sign of the two-mode squeezing parameter induced by the 0PN and 1PN couplings. We show that this behavior persists, and can be controlled, by varying the degree of squeezing of the initial states. We conclude by arguing that analogous cancellations of quantum correlations, where the system tends toward classicalization, should appear also in any other quantum mechanical theory of gravity.

## II. QUANTUM GRAVITATIONAL POTENTIAL AND HARMONIC OSCILLATORS

We consider the simple 1D toy model of two identical harmonic oscillators, A and B, characterized by the mass  $m$  and angular frequency  $\omega_m$ , oscillating along the  $x$ -axis. We will assume that the centres of the two harmonic traps are separated by a distance  $d$ , and the two particles interact only gravitationally. Using Gupta's framework of linearized quantum gravity [18,19] and perturbation theory, we can then obtain the gravitational matter-matter potential up to order 2PN [7] (see also [8–10])

$$\hat{H}_{\text{grav}} = -\frac{Gm^2}{|\hat{r}_A - \hat{r}_B|} - \frac{G(3\hat{p}_A^2 - 8\hat{p}_A\hat{p}_B + 3\hat{p}_B^2)}{2c^2|\hat{r}_A - \hat{r}_B|} + \frac{G(5\hat{p}_A^4 - 18\hat{p}_A^2\hat{p}_B^2 + 5\hat{p}_B^4)}{8c^4m^2|\hat{r}_A - \hat{r}_B|}, \quad (1)$$

where  $c$  ( $G$ ) denotes the speed of light (the gravitational constant). Here, we will implicitly assume that the momenta are sufficiently small such that higher order terms, i.e., the terms  $\propto \hat{p}_j^n \hat{p}_k^{n'}$  (with  $j, k = A, B$  and  $n + n' > 4$ ), can be neglected. Higher order terms would only modify the quantitative results for relativistic momenta without affecting the features in the regime where the velocities are small compared to the speed of light [i.e., we neglect terms beyond  $\mathcal{O}(c^{-4})$ ]. To keep the expressions short, we also implicitly assume the convention that unsymmetrized expressions (e.g.,  $\hat{x}\hat{p}$ ) are to be interpreted in the symmetrized ordering (e.g.,  $(\hat{x}\hat{p} + \hat{p}\hat{x})/2$ ).

Post-Newtonian corrections have, of course, been analyzed extensively in previous works in the center of momentum frame [2,3,5,6,29]. If we set  $\hat{p} \equiv \hat{p}_A = -\hat{p}_B$ , and denote  $\hat{r} \equiv |\hat{r}_A - \hat{r}_B|$ , we recover from Eq. (1) the known result in the literature

$$\hat{H}_{\text{grav}} = -\frac{Gm^2}{\hat{r}} - 7\frac{G\hat{p}^2}{c^2\hat{r}} - \frac{G\hat{p}^4}{c^4m^2\hat{r}}. \quad (2)$$

In other words, Eq. (1) can be seen as the adaptation of Eq. (2) to the specific case of two quantum harmonic oscillators. Generalizations to more particles, e.g., four harmonic oscillators, forming pairs of particles and detectors [30], modified gravity scenarios such as in the case of a massive graviton [10], fat graviton with nonlocal interaction [9,31], or a dilaton-graviton combination [32], can also be analyzed using similar methods.

We now suppose that the two trap centres are located at  $\pm d/2$  and write  $\hat{r}_A = -d/2 + \hat{x}_A$ , and  $\hat{r}_B = d/2 + \hat{x}_B$ . The operators  $\hat{x}_A$  and  $\hat{x}_B$  denote small displacements from the equilibrium position, while the corresponding conjugate momenta are given by  $\hat{p}_A$  and  $\hat{p}_B$ , respectively. The Hamiltonian of the two harmonic oscillators is given by

$$\hat{H}_{\text{matter}} = \frac{\hat{p}_A^2}{2m} + \frac{\hat{p}_B^2}{2m} + \frac{m\omega_m^2}{2}\hat{x}_A^2 + \frac{m\omega_m^2}{2}\hat{x}_B^2, \quad (3)$$

where  $\omega_m$  and  $m$  denote the harmonic frequency and mass, respectively (assumed for simplicity to be the same for the two harmonic oscillators). For later convenience, we introduce the mode decompositions

$$\hat{x}_A = \delta x(\hat{a} + \hat{a}^\dagger), \quad \hat{x}_B = \delta x(\hat{b} + \hat{b}^\dagger), \quad (4)$$

$$\hat{p}_A = i\delta p(\hat{a}^\dagger - \hat{a}), \quad \hat{p}_B = i\delta p(\hat{b}^\dagger - \hat{b}), \quad (5)$$

where  $\hat{a}, \hat{b}$  ( $\hat{a}^\dagger, \hat{b}^\dagger$ ) denote the annihilation (creation) operators, and  $\delta x = \sqrt{\frac{\hbar}{2m\omega_m}}$ ,  $\delta p = \sqrt{\frac{\hbar m\omega_m}{2}}$  are the position, momentum zero-point-motions, respectively.

Here, we will be interested in the phenomenology of the gravitational potential in Eq. (1) up to the quartic order in the operators  $\propto \hat{O}_i \hat{O}_j \hat{O}_k \hat{O}_l$  (with  $\hat{O}_{i,j,k,l} = \hat{x}_A, \hat{x}_B, \hat{p}_A, \hat{p}_B$ ) corresponding to small position and momentum fluctuations. Taylor expanding Eq. (1) around the equilibrium positions and considering small fluctuations, we find the following Hamiltonian:

$$\hat{H}_{\text{grav}} = -\frac{Gm^2}{d} + \hat{H}_A + \hat{H}_B + \hat{H}_{AB}, \quad (6)$$

where the first term only produces a global phase, and  $\hat{H}_A$  and  $\hat{H}_B$  depend only on the operators of particle A and B, respectively. The leading order cross-coupling terms between the two particles are given by

$$\hat{H}_{AB} = \frac{Gm^2}{d} \left[ \frac{2\hat{x}_A\hat{x}_B}{d^2} + \frac{4\hat{p}_A\hat{p}_B}{m^2c^2} - \frac{9\hat{p}_A^2\hat{p}_B^2}{4m^4c^4} \right], \quad (7)$$

where the 0PN, 1PN, and 2PN contributions appear from left to right, respectively.

While the leading order gravitational force arises from the terms  $\hat{H}_A$  and  $\hat{H}_B$  (as these terms contain the uniform gravitational fields affecting the motion of the individual particle), the leading order contribution for entanglement generation arises from the cross-couplings in  $\hat{H}_{AB}$  [33]. This is already hinting that the generation of gravitationally induced entanglement might be hiding some surprises.

### III. GRAVITATIONAL ENTANGLEMENT ENTROPY

In this section we illustrate how the gravitational entanglement entropy depends on the delocalization using simple first order perturbation theory. We assume that the initial state is a product of the two ground states

$$|\psi_i\rangle = |0\rangle_A |0\rangle_B, \quad (8)$$

which is perturbed by the gravitational interaction  $\hat{H}_{\text{grav}}$  in Eq. (6). We can always decompose the perturbed state vector in the number basis

$$|\psi_{AB}\rangle = \frac{1}{\sqrt{\mathcal{N}}} \sum_{n,N} C_{nN} |n\rangle |N\rangle, \quad (9)$$

where  $C_{nN}$  denote the coefficients (with  $C_{00} = 1$ ),  $\mathcal{N} = \sum_{n,N} |C_{nN}|^2$  is the normalization, and  $|n\rangle, |N\rangle$  denote the number states of the two harmonic oscillators. In particular, the coefficients appearing in Eq. (9) can be computed using

$$C_{nN} = \frac{\langle n | \langle N | \hat{H}_{AB} | 0 \rangle | 0 \rangle}{2E_0 - E_n - E_N}, \quad (10)$$

where  $E_0$  and  $E_n, E_N$  denote the energy of the ground state  $|0\rangle$  and of the excited states  $|n\rangle, |N\rangle$ , respectively (we recall that for a harmonic oscillator, we have  $E_j = E_0 + \hbar\omega j$  with  $j$  denoting the occupation number).

We will quantify the degree of entanglement using the von Neumann entanglement entropy given by  $S = -\text{tr}[\rho_A \ln \rho_A]$ , where  $\rho_A = \text{tr}_B[\rho_{AB}]$  is the reduced density matrix of subsystem A, and  $\rho_{AB} = |\psi_{AB}\rangle \langle \psi_{AB}|$  is the total density matrix of the system (see Appendix A for a short review on the entanglement entropy). Using Eqs. (7)–(10) find a simple formula for the steady-state entanglement entropy

$$S \approx -\left(\frac{Gm}{c^2 d} - \frac{Gm}{2d^3 \omega_m^2}\right)^2 \log\left(\left(\frac{Gm}{c^2 d} - \frac{Gm}{2d^3 \omega_m^2}\right)^2\right) - \frac{81G^2 \omega_m^2 \hbar^2}{1024c^8 d^2} \log\left(\frac{81G^2 \omega_m^2 \hbar^2}{1024c^8 d^2}\right), \quad (11)$$

which is plotted in Fig. 1 (see Appendix B for the detailed derivation). The first line of Eq. (11) captures the rightmost part of the plot (from the 0PN  $\hat{x}_A \hat{x}_B$  coupling) as well as the plateau (from the 1PN  $\hat{p}_A \hat{p}_B$  coupling). The rightmost

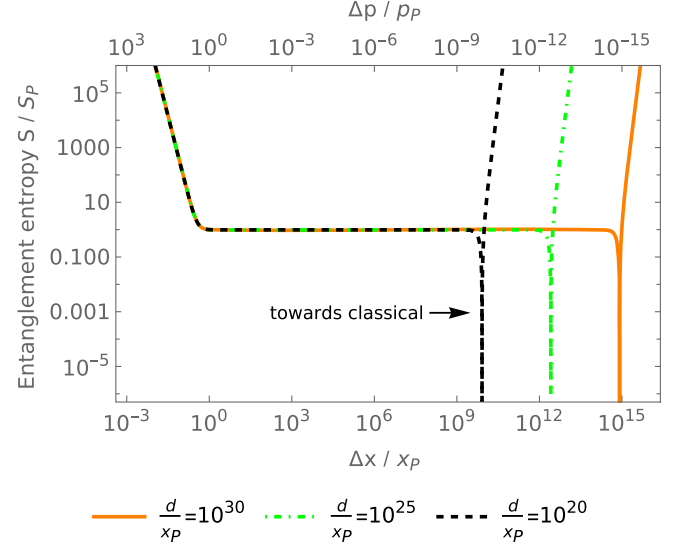


FIG. 1. Entanglement entropy  $S$  as a function of the spatial delocalization  $\Delta x$  (bottom) or the momentum delocalization  $\Delta p = \hbar/\Delta x$  (top). We have expressed the spatial (momentum) superposition in units of the Planck length (momentum) given by  $x_P \equiv \sqrt{\hbar G/c^3}$  ( $p_P \equiv \hbar/x_P$ ). The behavior on the right is determined by the static contribution  $\propto \hat{x}_A \hat{x}_B$ . The plateau in the middle is determined by the nonstatic 1PN contribution  $\propto \hat{p}_A \hat{p}_B$ . The dominant static and the nonstatic couplings cancel each other's contribution to the entanglement entropy at  $\sqrt{2}d\omega_m \sim c$ , and we observe that the entanglement entropy  $S$  drops to negligible values (the three pronounced dips indicated by the arrow). We note that these dips of quantum correlations indicate a *classicalization* of the system and that they occur far from the Planck length  $x_P$ . Finally, as we approach relativistic velocities (corresponding to large momentum superposition sizes on the left side of the figure), we find that higher-order momentum contributions become important. Here we have plotted the contribution from the term  $\propto \hat{p}_A^2 \hat{p}_B^2$  arising at order  $\mathcal{O}(1/c^4)$ . We plot the curves for different values of the trap distance  $d$ . Note that the qualitative behavior remains the same in all three cases, with the location of the dip shifting to the left (right) for smaller (larger) values of  $d$  as expected (i.e., larger distances weaken the position couplings, hence requiring larger spatial superposition sizes). The entanglement entropy is expressed in units of the entanglement entropy when we set the spatial superposition to that of the Planck length, i.e.,  $S_P = S(\Delta x = x_P) = -(\frac{Gm}{c^2 d})^2 \log((\frac{Gm}{c^2 d})^2)$  which is achieved on the plateau.

part of the plot in Fig. 1 is captured by the 2PN contribution in the second line of Eq. (11) arising from the coupling  $\propto \hat{p}_A^2 \hat{p}_B^2$ .

We find that the entanglement entropy grows for very large and very small positions delocalizations  $\Delta x$  given by the zero-point-motion. For large  $\Delta x$  the entanglement entropy grows as a consequence of the 0PN static position couplings arising from the familiar  $1/r$  potential, while for small  $\Delta x$  the momentum delocalization  $\Delta p \sim \hbar/\Delta x$  becomes large, and the post-Newtonian momentum couplings start increasing the entanglement entropy. In other words, the landscape of entanglement entropy as a function of delocalizations  $\Delta x$  or  $\Delta p$  forms a valley. This can be

seen as a consequence of Heisenberg's minimum uncertainty relation  $\Delta p \Delta x = \hbar/2$  and the universal coupling of gravity to all forms of energy.

In addition, Fig. 1 reveals unexpected dips in entanglement entropy, which appear far the Planck length. These dips arise because of the cancellation between the OPN and 1PN terms in the first line of Eq. (11) corresponding to the couplings  $\propto \hat{x}_A \hat{x}_B$  and  $\propto \hat{p}_A \hat{p}_B$ , respectively. The first line vanishes when the product of the harmonic frequency,  $\omega_m$ , and of the distance between the two traps,  $d$ , becomes comparable to the speed of light, i.e.,  $\sqrt{2}\omega_m d = c$ . In this case, the position and momentum delocalizations are given by  $\Delta x = \sqrt{\frac{\hbar d}{mc}}/\sqrt[4]{2}$  and  $\Delta p = \sqrt{\frac{\hbar mc}{d}}/\sqrt[4]{2}$ , respectively. At this point, the two adimensional parameters governing the OPN and 1PN match, i.e.,  $\Delta x/d = \sqrt{2}\Delta p/(mc)$ .

The adimensional parameters however only explain that the OPN and 1PN contributions are of equal magnitude without revealing the origin of the cancellation. As we will see in the next section, this cancellation arises from the opposite sign of the two-mode squeezing (TMS) character of the position and momentum couplings.

#### IV. DIPS OF GRAVITATIONAL ENTANGLEMENT

In this section we look closer at the unexpected dips of gravitational entanglement uncovered in the previous section. We restrict the analysis only to the leading order terms identified in the previous section as its origin, i.e.,

$$\hat{H}_{AB} = \frac{2Gm^2}{d^3} \hat{x}_A \hat{x}_B + \frac{4G}{c^2 d} \hat{p}_A \hat{p}_B. \quad (12)$$

Using Eqs. (4) and (5) in Eq. (12) we then find

$$\hat{H}_{AB} = \hbar g_- (\underbrace{\hat{a} \hat{b} + \hat{a}^\dagger \hat{b}^\dagger}_{\text{TMS}}) + \hbar g_+ (\underbrace{\hat{a} \hat{b}^\dagger + \hat{a}^\dagger \hat{b}}_{\text{BS}}), \quad (13)$$

where the coupling rates are

$$g_- = g_x - g_p, \quad g_+ = g_x + g_p, \quad (14)$$

$$g_x = \frac{Gm}{d^3 \omega_m}, \quad g_p = \frac{2Gm\omega_m}{c^2 d}, \quad (15)$$

and TMS (BS) labels the two-mode squeezing (beam-splitter) contribution (for an introduction on quantum optics transformations see for example [34,35]).

For an initial product of ground states  $|0\rangle|0\rangle$  the BS part of the Hamiltonian has no effect, while the TMS-induced change depends on the PN order: at OPN we have the coupling  $+g_x$ , while at 1PN we have the coupling  $-g_p$ . The explanation for the dips in Fig. 1 thus lies in the opposite sign of the TMS transformation arising from the position and momentum couplings of gravity. When  $g_x = g_p$  the

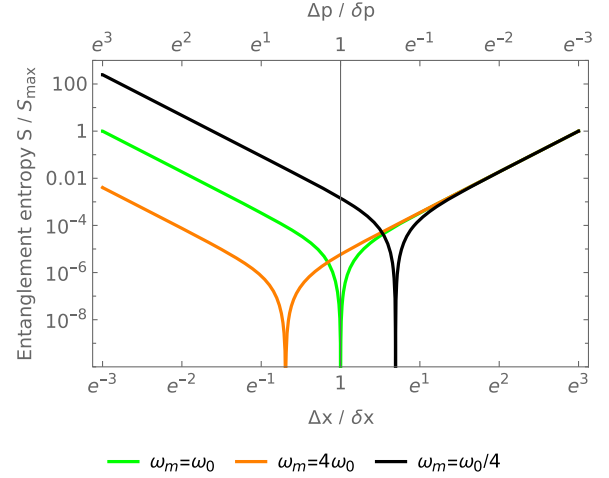


FIG. 2. The maximum entanglement value achieved during the time evolution starting with a product of two single-mode-squeezed-vacuum (SMSV) states as a function of the spatial delocalization  $\Delta x = \delta x e^{-r}$  (bottom axis) and momentum delocalization  $\Delta p = \delta p e^r$  (top axis). By setting  $\omega_m = \omega_0 \equiv c/(\sqrt{2}d)$  we find the case of equal couplings  $g_x = g_p = g_0 \equiv \sqrt{2}Gm/(c^2 d)$  (green line). We also consider the case  $\omega_m = 4\omega_0$  producing the couplings  $4g_x = g_p/4 = g_0$  (orange line), and the case  $\omega_m = \omega_0/4$  producing the coupling  $g_x/4 = 4g_p = g_0$  (black line). The entanglement entropy is normalized to the maximum value of the green line to ease the comparison. We note that both the horizontal location and the depth can be changed by tuning the couplings  $g_x, g_p$  using the mechanical frequency  $\omega_m$ . At the location of the dips the system tends toward classicalization as there is a strong suppression of quantum correlations.

OPN and 1PN contributions to TMS cancel, i.e.,  $g_- = 0$ , and we find a dip.

The observed cancellation point persists even if we consider the initial state to be the product of two single-mode-squeezed-vacuum (SMSV) states which have enhanced position or momentum delocalizations given by

$$\Delta x = \delta x e^{-r}, \quad \Delta p = \delta p e^r, \quad (16)$$

respectively [with  $\delta x$  and  $\delta p$  denoting the zero-point-motions defined below Eq. (5)]. Such states are not energy eigenstates, and hence, we have to take into account their time-evolution in the harmonic traps (see derivation in Appendix C). In Fig. 2 we show how the maximum achieved entanglement entropy changes by varying the degree of squeezing  $r$  of the initial state. We note that by tuning the mechanical frequency  $\omega_m$  [and hence the couplings  $g_x, g_p$  in Eq. (14)] we can also shift to profile horizontally and increase its depth. The location of the dip is now determined by the condition  $g_x e^{-2r} = g_p e^{2r}$ , which depends on the squeezing parameter  $r$  as expected.



## V. DISCUSSION

In this work, we have discussed entanglement generation within the context of a linearized quantum gravity with post-Newtonian (PN) momentum contributions. We have considered a simple toy model of two nearby harmonic oscillators and computed the entanglement entropy arising from their gravitational interaction. We uncovered a surprising interplay between the Heisenberg's uncertainty relation, the quantum squeezing character of gravity, and the generation of nonclassical correlations when 1PN and 2PN contributions are taken into account. Other effects, such as gravitational radiation [36] and radiation reaction [37], could however provide significant channels for loss of coherence at relativistic speeds when higher order PN effects become important. We leave a systematic exploration of the balance between gravitationally induced entanglement and decoherence at different PN orders for future work.

In summary, we found that the entanglement entropy drops to negligible values when the 0PN contribution and the 1PN are of the same magnitude, i.e., when  $\Delta x/d \sim \Delta p/(mc)$ , where  $m$  is the mass of each harmonic oscillator, and  $d$  denotes the distance between the two trap centers. Although the classical gravitational force is universally attractive, the generation of gravitationally induced entanglement can be suppressed to negligible values for specific states. As this will remain true within any theory that recovers the predictions of perturbative quantum gravity, such states could provide a method to distinguish perturbative quantum gravity from other classes of gravitational theories, such as a scalar-tensor theory with different PN contributions. While this work does not answer questions of experimental feasibility, it nonetheless uncovers experimentally defining features of infrared quantum gravity. The entanglement dips provide a distinct signature of classicalization, showing how quantum correlations can become suppressed in a fully quantum mechanical framework.

## ACKNOWLEDGMENTS

M.T. acknowledges funding from Grant No. ST/W006227/1 and the Slovenian Research and Innovation Agency (ARIS) under Contracts No. N1-0392, No. P1-0416, No. SN-ZRD/22-27/0510 (RSUL Toroš). M.S. is supported by the Fundamentals of the Universe research program at the University of Groningen. P.A. acknowledges funding from Brazilian Coordination for the Improvement of Higher Education Personnel (CAPES), Erasmus + Programme and the Strategic Partnership Framework at University of Groningen. S.B. thanks EPSRC Grants No. EP/R029075/1, No. EP/X009467/1, and No. ST/W006227/1. S.B. and A.M.'s research is supported by the Sloan, and Betty and Moore foundations.

## APPENDIX A: BRIEF OVERVIEW OF ENTANGLEMENT ENTROPY FORMULAS

The von Neumann entanglement entropy is given by

$$S = -\text{tr}[\rho_A \ln \rho_A], \quad (\text{A1})$$

where  $\rho_A = \text{tr}_B[\rho_{AB}]$  is the reduced density matrix of subsystem A,  $\rho_{AB} = |\psi_{AB}\rangle\langle\psi_{AB}|$  is the total density matrix of the system. The same form of the expression would be obtained by tracing over system A by formally exchanging the subsystems A and B, i.e.,  $S = -\text{tr}[\rho_B \ln \rho_B]$  and  $\rho_B = \text{tr}_A[\rho_{AB}]$ . The general expression in Eq. (A1) can be however rewritten in a more convenient way for the two cases we analyse in Secs. III and IV.

In Sec. III, we will suppose that the initial state is the product of the ground states of two harmonic oscillators, i.e.,  $|0\rangle|0\rangle$  and use time-independent perturbation theory. Using the Schmidt decomposition of the state in Eq. (9) it can be shown that the entanglement entropy from Eq. (A1) reduces to

$$S = -\sum_j |\alpha_j|^2 \log[|\alpha_j|^2], \quad (\text{A2})$$

where  $\alpha_j$  are the Schmidt coefficients. The Schmidt decomposition can, in general, be performed using the linear algebra technique of singular value decomposition (SVD) [38]. However, we will be primarily interested in the states of the form  $\sum_j \alpha_j |j\rangle|j\rangle$  (with  $|j\rangle$  denoting the number states), where one can readily read off the Schmidt coefficients  $\alpha_j$ .

In Sec. IV, we will be interested in Gaussian states and their time-evolution. The formula for the entanglement entropy simplifies to [39–43]

$$S = -f \ln f + (1+f)(1+\ln f), \quad (\text{A3})$$

where  $f(t)$  is the symplectic eigenvalue of the single-mode covariance matrix of subsystem A given by

$$f(t) = \frac{1}{\hbar} \sqrt{4\langle\hat{x}_A^2\rangle\langle\hat{p}_A^2\rangle - \langle\hat{x}_A\hat{p}_A + \hat{p}_A\hat{x}_A\rangle^2} - \frac{1}{2}. \quad (\text{A4})$$

Also, the formula in Eq. (A3) remains valid if we formally replace the quantities related to subsystem A with the ones for subsystem B in Eq. (A4) (i.e., we compute the symplectic eigenvalue of the single mode covariance matrix of subsystem B).

## APPENDIX B: LIST OF EXPANSION COEFFICIENTS UP TO QUARTIC ORDER IN THE OPERATORS AND UP TO 2PN

From Eq. (1) we find that the cross-coupling terms between the two particles are given by

TABLE I. List of all gravitational couplings up to quartic order in operators and up to order 2PN (first three columns). Using first-order perturbation theory in Eq. (10) we obtain the 25 nonzero coefficients  $C_{nN}$  in columns four to nine (the coefficients  $C_{0N}$  and  $C_{n0}$  will not contribute to the entanglement at first order in perturbation theory and are left out of the table [33]). The *local dip feature* in the generation of entanglement occurs as a result of the cancellation arising from the terms  $\propto \hat{x}_A \hat{x}_B$  and  $\propto \hat{p}_A \hat{p}_B$ . As discussed in the main text, this is a result of the different signs of the induced two-mode-squeezing (TMS) transformation from the leading order 0PN and 1PN terms with the hint in the different sign of the corresponding  $C_{11}$  coefficients. We note that additional cancellations occur in every column; we see that the  $C_{nN}$  coefficients in all columns have both positive and negative values. The *broad valley feature* can be understood directly from the couplings. On the one hand, for large-position delocalization  $\Delta x$  the 0PN term  $\propto \hat{x}_A \hat{x}_B$  generates a rapid increase of the entanglement entropy with increasing  $\Delta x$ , and, on the other hand, for large momentum delocalization  $\Delta p$  (i.e., tiny spatial delocalization) the term  $\propto \hat{p}_A^2 \hat{p}_B^2$  also produces a fast growth of the entanglement entropy with increasing  $\Delta p$ . In other words, entanglement entropy as function of position delocalization is loosely speaking “U” shaped, forming a valley of entanglement.

Order	Coefficient	Coupling	Nonzero coefficients $C_{nN}$ from first-order perturbation theory					
			$C_{11}$	$C_{21}$	$C_{12}$	$C_{31}$	$C_{13}$	$C_{22}$
0PN	$\frac{2Gm^2}{d^3}$	$\hat{x}_A \hat{x}_B$	$-\frac{Gm}{2d^3 \omega_m^2}$					
	$\frac{3Gm^2}{d^4}$	$\hat{x}_A^2 \hat{x}_B$		$-\frac{Gm\delta x}{\sqrt{2}d^4 \omega_m^2}$				
	$-\frac{3Gm^2}{d^4}$	$\hat{x}_A \hat{x}_B^2$			$\frac{Gm\delta x}{\sqrt{2}d^4 \omega_m^2}$			
	$\frac{4Gm^2}{d^5}$	$\hat{x}_A^3 \hat{x}_B$	$-\frac{3Gh}{2d^5 \omega_m^3}$			$-\frac{\sqrt{6}Gh}{4d^5 \omega_m^3}$		
	$-\frac{6Gm^2}{d^5}$	$\hat{x}_A^2 \hat{x}_B^2$						$\frac{3Gh}{4d^5 \omega_m^3}$
	$\frac{4Gm^2}{d^5}$	$\hat{x}_A \hat{x}_B^3$	$-\frac{3Gh}{2d^5 \omega_m^3}$				$-\frac{\sqrt{6}Gh}{4d^5 \omega_m^3}$	
1PN	$\frac{4G}{c^2 d}$	$\hat{p}_A \hat{p}_B$	$\frac{Gm}{c^2 d}$					
	$\frac{4G}{c^2 d^2}$	$\hat{p}_A \hat{p}_B \hat{x}_A$		$\frac{2\sqrt{2}Gm\delta x}{3c^2 d^2}$				
	$-\frac{4G}{c^2 d^2}$	$\hat{p}_A \hat{p}_B \hat{x}_B$			$-\frac{2\sqrt{2}Gm\delta x}{3c^2 d^2}$			
	$\frac{4G}{c^2 d^3}$	$\hat{p}_A \hat{p}_B \hat{x}_A^2$	$\frac{Gh}{2c^2 d^3 \omega_m}$			$\frac{\sqrt{6}Gh}{4c^2 d^3 \omega_m}$		
	$-\frac{8G}{c^2 d^3}$	$\hat{p}_A \hat{p}_B \hat{x}_A \hat{x}_B$						$-\frac{Gh}{c^2 d^3 \omega_m}$
	$\frac{4G}{c^2 d^3}$	$\hat{p}_A \hat{p}_B \hat{x}_B^2$	$\frac{Gh}{2c^2 d^3 \omega_m}$				$\frac{\sqrt{6}Gh}{4c^2 d^3 \omega_m}$	
	$\frac{3G}{2c^2 d^2}$	$\hat{p}_A^2 \hat{x}_B$		$\frac{\sqrt{2}Gm\delta x}{4c^2 d^2}$				
	$-\frac{3G}{2c^2 d^2}$	$\hat{p}_A^2 \hat{x}_B^2$						$-\frac{3Gh}{16c^2 d^3 \omega_m}$
	$\frac{3G}{c^2 d^3}$	$\hat{p}_A^2 \hat{x}_A \hat{x}_B$	$-\frac{3Gh}{8c^2 d^3 \omega_m}$			$\frac{3\sqrt{6}Gh}{16c^2 d^3 \omega_m}$		
	$\frac{3G}{2c^2 d^2}$	$\hat{p}_B^2 \hat{x}_A$			$\frac{\sqrt{2}Gm\delta x}{4c^2 d^2}$			
	$-\frac{3G}{2c^2 d^2}$	$\hat{p}_B^2 \hat{x}_A^2$						$-\frac{3Gh}{16c^2 d^3 \omega_m}$
	$\frac{3G}{c^2 d^3}$	$\hat{p}_B^2 \hat{x}_B \hat{x}_A$	$-\frac{3Gh}{8c^2 d^3 \omega_m}$				$\frac{3\sqrt{6}Gh}{16c^2 d^3 \omega_m}$	
2PN	$-\frac{9G}{4c^4 m^2 d}$	$\hat{p}_A^2 \hat{p}_B^2$						$\frac{9Gh\omega_m}{32c^4 d}$

$$\begin{aligned}
\Delta \hat{H}_{AB} = & \frac{Gm^2}{d^3} \left( 2\hat{x}_A \hat{x}_B + 3 \frac{(\hat{x}_A^2 \hat{x}_B - \hat{x}_A \hat{x}_B^2)}{d} \right. \\
& \left. + \frac{4\hat{x}_A^3 \hat{x}_B - 6\hat{x}_A^2 \hat{x}_B^2 + 4\hat{x}_A \hat{x}_B^3}{d^2} \right) \\
& + \frac{G}{c^2 d} \left( 4\hat{p}_A \hat{p}_B \left( 1 + \frac{\hat{x}_A - \hat{x}_B}{d} + \frac{(\hat{x}_A - \hat{x}_B)^2}{d^2} \right) \right. \\
& + \frac{3\hat{p}_A^2}{2} \left( \frac{\hat{x}_B}{d} + \frac{2\hat{x}_A \hat{x}_B - \hat{x}_B^2}{d^2} \right) \\
& \left. + \frac{3\hat{p}_B^2}{2} \left( \frac{\hat{x}_A}{d} + \frac{2\hat{x}_A \hat{x}_B - \hat{x}_A^2}{d^2} \right) \right) - \frac{9G}{4c^4 m^2 d} \hat{p}_A^2 \hat{p}_B^2,
\end{aligned} \tag{B1}$$

where the first two lines contain the static limit 0PN contribution, lines three to five contain the 1PN contribution and the last term corresponds to the 2PN contribution. While the leading order gravitational force arises from the terms  $\hat{H}_A$  and  $\hat{H}_B$  (as these terms contain the uniform gravitational fields affecting the motion of the individual particle), the leading order contribution for entanglement generation arises from the cross-couplings in  $\hat{H}_{AB}$ .

In Table I, we have listed the couplings from Eq. (7) and applied Eq. (10) to obtain the nonzero expansion coefficient  $C_{nN}$  for  $n, N > 0$  (the coefficients  $C_{0N}$  and  $C_{n0}$  will not contribute to the entanglement at first order in perturbation theory and are left out of the computation). The resulting entanglement entropy computed using Eq. (A2) as a

function of position delocalization  $\Delta x \equiv \delta x$  (bottom axis) and momentum delocalization  $\Delta p \equiv \delta p = \hbar/\Delta x$  (top axis) is plotted in Fig. 1.

We can, however, capture both qualitatively and quantitatively the entanglement entropy shown in Fig. 1 by considering only three couplings from Table I. In the rightmost part of the figure, the momentum couplings (1PN and 2PN effects) are negligible as the momentum delocalization  $\Delta p$  is tiny compared to  $mc$ , and hence dominated by the position 0PN couplings. Furthermore, if the size of the delocalization  $\Delta x$  is also small compared to the distance between the traps  $d$ , then we can further neglect the cubic and quartic couplings, leaving us with the coupling  $\propto \hat{x}_A \hat{x}_B$ . The intermediate plateau is captured by the 1PN coupling  $\propto \hat{p}_A \hat{p}_B$  as the ratio  $\Delta x/d$  becomes tiny, and  $\Delta p$  becomes non-negligible compared to  $mc$ . Finally, the leftmost part of the figure is dominated by the 2PN coupling  $\propto \hat{p}_A^2 \hat{p}_B^2$ , and eventually by higher order PN corrections as we would further increase  $\Delta p$ . By making such simplifications, the perturbed state can be written as

$$|\psi_{AB}\rangle \approx \frac{1}{\mathcal{N}} [ |0\rangle|0\rangle - C_{11}|1\rangle|1\rangle - C_{22}|2\rangle|2\rangle ], \quad (\text{B2})$$

where  $|0\rangle, |1\rangle, |2\rangle$  denote the number states, and  $\mathcal{N}$  denotes the overall normalization. To compute the entanglement entropy in Eq. (11), we can now readily use Eq. (A2), where we can make the further approximation  $\mathcal{N} \approx 1$  as we have  $C_{00} \approx 1$  and  $C_{11}, C_{22} \ll 1$  (while the terms  $C_{11}^2, C_{22}^2$  appearing in  $\mathcal{N}$  would only contribute higher order corrections).

Let us briefly comment how to see the entanglement dip from Table I. We first recall that the TMS operator can be written in the form  $\widehat{S}(\xi) = \exp(-i(\xi^* \hat{a} \hat{b} + \xi \hat{a}^\dagger \hat{b}^\dagger))$ , where the TMS generator is  $\propto \xi^* \hat{a} \hat{b} + \xi \hat{a}^\dagger \hat{b}^\dagger$ . From Eq. (10) we immediately find

$$C_{nN} \propto \langle n | \langle N | \hat{H}_{AB} | 0 \rangle | 0 \rangle \propto \pm \langle n | \langle N | \hat{a}^\dagger \hat{b}^\dagger + \hat{a} \hat{b} | 0 \rangle | 0 \rangle, \quad (\text{B3})$$

with the plus (minus) sign corresponding to the 0PN coupling  $\hat{x}_A \hat{x}_B$  (1PN coupling  $\hat{p}_A \hat{p}_B$ ). In other words, the 0PN position coupling would like to squeeze with TMS parameter  $\xi = +1$  while the 1PN momentum coupling would like to squeeze in the opposite direction with TMS parameter  $\xi = -1$ . The 0PN and 1PN two-mode squeezing contributions cancel when  $\Delta x/d = \sqrt{2} \Delta p/(mc)$ . Summing the two contributions, we find a total squeezing parameter  $\xi = 0$  and a suppression of the gravitationally induced entanglement. The reason for the entanglement suppression thus lies in the opposite sign of the two-mode squeezing (TMS) parameter at the leading order 0PN and 1PN gravitational interaction.

## APPENDIX C: DERIVATION OF THE TIME-DEPENDENT ENTANGLEMENT ENTROPY

Here, we further explore the dip in entanglement generation by considering the initial state to be the product of two single-mode-squeezed-vacuum (SMSV) states

$$|\psi_i\rangle = |r\rangle_A |r\rangle_B, \quad (\text{C1})$$

where  $r \in \mathbb{R}$  is the SMSV squeezing parameter. The single mode squeezed state is given by

$$|r\rangle = \frac{1}{\sqrt{\cosh r}} \sum_{n=0}^{\infty} (\tanh r)^n \frac{\sqrt{(2n)!}}{2^n n!} |2n\rangle, \quad (\text{C2})$$

where  $|n\rangle$  denotes the number state of the considered harmonic oscillator. The state in Eq. (C2) has enhanced position or momentum delocalization is given by

$$\Delta x = \delta x e^{-r}, \quad \Delta p = \delta p e^r, \quad (\text{C3})$$

respectively [with  $\delta x$  and  $\delta p$  denoting the zero-point-motions defined below Eq. (5)]. Such states are not energy eigenstates, and hence, we have to take into account their time-evolution in the harmonic traps. However, as the initial state in Eq. (C1) is Gaussian, and the interaction in Eq. (12) is quadratic in the operators, the state will remain Gaussian also at any later time.

The Heisenberg equations of motion for the modes of the harmonic oscillators evolve as [44]

$$\hat{a}(t) = c_0(t) \hat{a} + c_+(t) \hat{b} + c_-(t) \hat{b}^\dagger, \quad (\text{C4})$$

$$\hat{b}(t) = c_0(t) \hat{b} - c_+(t) \hat{a} - c_-(t) \hat{a}^\dagger, \quad (\text{C5})$$

where  $\hat{a} \equiv \hat{a}(0)$ ,  $\hat{b} \equiv \hat{b}(0)$ . The time-dependent coefficients are given by [44]

$$c_0(t) = \cos(\omega_e t) - i \frac{\omega_m}{\omega_e} \sin(\omega_e t), \quad (\text{C6})$$

$$c_{\pm}(t) = g_{\pm} \frac{\omega_m}{\omega_e} \sin(\omega_e t), \quad (\text{C7})$$

where we have defined the effective frequency  $\omega_e = \sqrt{\omega_m^2 + g_+^2 - g_-^2}$ . We can now readily compute the time dependency of the entanglement entropy. Inserting Eq. (C4) in Eq. (A4) we find that the problem reduces to evaluating the expectation values of the initial state in Eq. (C1). In particular, to complete the analysis, we use the following expectation values [34,35]:

$$\langle \hat{a} \hat{a} \rangle = \langle \hat{b} \hat{b} \rangle = -\sinh(r) \cosh(r), \quad (\text{C8})$$

$$\langle \hat{a}^\dagger \hat{a}^\dagger \rangle = \langle \hat{b}^\dagger \hat{b}^\dagger \rangle = -\sinh(r) \cosh(r), \quad (\text{C9})$$

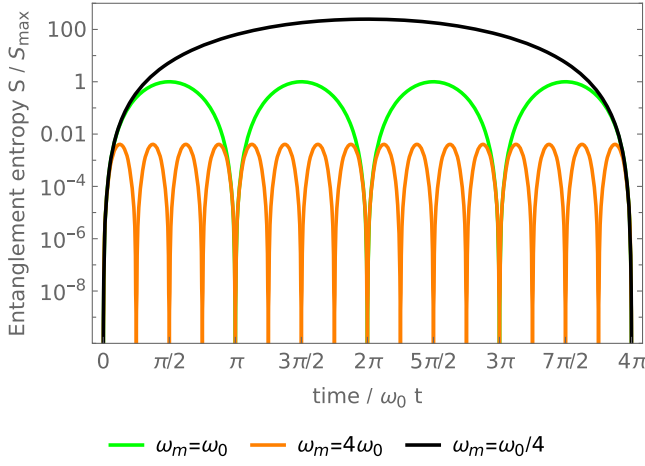


FIG. 3. Entanglement entropy  $S$  as a function of time  $t$  for different values of the couplings  $g_x, g_p$  defined in Eq. (14) (which scale as a function of the harmonic frequency  $\omega_m$ ). The SMSV squeezing parameter is set to  $r = -3$  corresponding to initial position squeezing  $\Delta x = \delta x e^{-r}$  and momentum delocalization  $\Delta p = \delta p e^r$ . By setting  $\omega_m = \omega_0 \equiv c/(\sqrt{2}d)$  we find the case of equal couplings  $g_x = g_p = g_0 \equiv \sqrt{2}Gm/(c^2d)$  (green line). We also consider the case  $\omega_m = 4\omega_0$  producing the couplings  $4g_x = g_p/4 = g_0$  (orange line), and the case  $\omega_m = \omega_0/4$  producing the coupling  $g_x/4 = 4g_p = g_0$  (black line). In all cases, the maximum entanglement is generated at  $\omega_m t = \pi/2$ . The entanglement entropy is normalized to the maximum value  $S_{\max}$  of the green curve to ease the comparison with Fig. 2.

$$\langle \hat{a} \hat{a}^\dagger \rangle = \langle \hat{b} \hat{b}^\dagger \rangle = \cosh^2(r), \quad (\text{C10})$$

$$\langle \hat{a}^\dagger \hat{a} \rangle = \langle \hat{b}^\dagger \hat{b} \rangle = \sinh^2(r), \quad (\text{C11})$$

where the expectation values are computed with respect to the SMSV state in Eq. (C2).

Inserting Eq. (A4) in Eq. (A3), and neglecting higher order terms in  $g_{x,p}/\omega_m$ , we eventually find the formula for the time-dependent entanglement entropy  $S(t)$

$$S(t) \approx -\frac{A(t)}{2\omega_m^2} \sin^2(\omega_m t) \left( \ln \left[ \frac{A(t)}{2\omega_m^2} \sin^2(\omega_m t) \right] - 1 \right). \quad (\text{C12})$$

where

$$A(t) = g_p^2 - 4g_p g_x + g_x^2 + (g_p^2 + g_x^2) \cos(2\omega_m t) + 2(g_p^2 e^{4r} + g_x^2 e^{-4r}) \sin^2(\omega_m t). \quad (\text{C13})$$

We analyze the temporal behavior of Eq. (C12) in Fig. 3. We first find that the behavior remains qualitatively similar as we change the frequency  $\omega_m$ . The entanglement entropy  $S(t)$  has the maximum at  $\omega_m t = \pi/2$  in all cases. Setting

$\omega_m t = \pi/2$  we find that the maximum entanglement increases both for  $r < 0$  (i.e., spatial delocalization  $\Delta x > \delta x$ ) as well as for  $r > 0$  (momentum delocalization  $\Delta p > \delta p$ ). This is not surprising as a squeezed state breaks the symmetry of the ground state, leaving it more exposed to TMS with either positive or negative values.

The generated entanglement becomes negligible when the condition  $A = 0$  is met [at  $t = \pi/(2\omega_m)$ ]. In this case we are in an entanglement dip, such that  $S(t) = 0 \forall t$ , as can be noted by computing the limit of Eq. (C12)

$$\lim_{A \rightarrow 0} S(t) = 0. \quad (\text{C14})$$

In particular, if we set  $t = \pi/(2\omega_m)$  in Eq. (C13), and impose  $A = 0$ , we find the simple condition for the location of the dip

$$g_x e^{-2r} = g_p e^{2r}. \quad (\text{C15})$$

If we set  $r = 0$  in Eq. (C15) we recover the condition  $g_x = g_p$  emerging at the level of the Hamiltonian in Eqs. (13) and (14) as highlighted in the main text. In other words, the squeezing effectively changes the quadratic position and momentum couplings resulting in the modified condition for the dip. We observe the shifted dip location according to Eq. (C15) in Fig. 2.

To summarize, the OPN position coupling  $\hat{x}_A \hat{x}_B$  and the 1PN momentum coupling  $\hat{p}_A \hat{p}_B$  induce two-mode squeezing (TMS) with an opposite sign of the squeezing parameter  $\xi$ . The OPN and 1PN coupling are a source of TMS with squeezing parameter  $\xi = +1$  and  $\xi = -1$ , which would individually generate TMS entangled states. However, when the two effects combine, they cancel, resulting in a strong suppression of gravitationally induced entanglement.

As a safety check, we consider the case where the position and momentum coupling match such that  $g_- = g_x - g_p$  vanishes, and we would thus expect a strong suppression of entanglement generation. We define

$$\omega_0 \equiv c/(\sqrt{2}d), \quad g_0 \equiv \sqrt{2}Gm/(c^2d), \quad (\text{C16})$$

and find that when  $\omega_m = \omega_0$  we have equal couplings  $g_x = g_p = g_0$ . Using this symmetric coupling regime, we find from Eq. (C13) a simplified expression.

$$A(t) \approx 8g_0^2 \sinh^2(2r) \sin^2(\omega_m t). \quad (\text{C17})$$

Setting  $\omega_m t = \pi/2$  and taking the limit  $r \rightarrow 0$  in Eq. (C12) with  $A(t)$  from Eq. (C17) we recover that the entanglement entropy vanishes (case corresponding to the dip found in Fig. 1 for the ground state).



- [1] Clifford M. Will, The confrontation between general relativity and experiment, *Living Rev. Relativity* **17**, 1 (2014).
- [2] Yoichi Iwasaki, Quantum theory of gravitation vs. classical theory: Fourth-order potential, *Prog. Theor. Phys.* **46**, 1587 (1971).
- [3] Kichiro Hiida and Hiroshi Okamura, Gauge transformation and gravitational potentials, *Prog. Theor. Phys.* **47**, 1743 (1972).
- [4] John F. Donoghue, General relativity as an effective field theory: The leading quantum corrections, *Phys. Rev. D* **50**, 3874 (1994).
- [5] Andrea Cristofoli, N. E. J. Bjerrum-Bohr, Poul H. Damgaard, and Pierre Vanhove, Post-Minkowskian Hamiltonians in general relativity, *Phys. Rev. D* **100**, 084040 (2019).
- [6] Gianluca Grignani, Troels Harmark, Marta Orselli, and Andrea Placidi, Fixing the non-relativistic expansion of the 1 pm potential, *J. High Energy Phys.* **10** (2020) 053.
- [7] Sougato Bose, Anupam Mazumdar, Martine Schut, and Marko Toroš, Mechanism for the quantum natured gravitons to entangle masses, *Phys. Rev. D* **105**, 106028 (2022).
- [8] Dripto Biswas, Sougato Bose, Anupam Mazumdar, and Marko Toroš, Gravitational optomechanics: Photon-matter entanglement via graviton exchange, *Phys. Rev. D* **108**, 064023 (2023).
- [9] Ulrich K. Beckering Vinckers, Álvaro de la Cruz-Dombriz, and Anupam Mazumdar, Quantum entanglement of masses with nonlocal gravitational interaction, *Phys. Rev. D* **107**, 124036 (2023).
- [10] Shafaq Gulzar Elahi and Anupam Mazumdar, Probing massless and massive gravitons via entanglement in a warped extra dimension, *Phys. Rev. D* **108**, 035018 (2023).
- [11] Sougato Bose, Anupam Mazumdar, Gavin W. Morley, Hendrik Ulbricht, Marko Toroš, Mauro Paternostro, Andrew Geraci, Peter Barker, M. S. Kim, and Gerard Milburn, Spin entanglement witness for quantum gravity, *Phys. Rev. Lett.* **119**, 240401 (2017).
- [12] Chiara Marletto and Vlatko Vedral, Gravitationally induced entanglement between two massive particles is sufficient evidence of quantum effects in gravity, *Phys. Rev. Lett.* **119**, 240402 (2017).
- [13] Sougato Bose, 2016, [https://www.youtube.com/watch?v=0Fv-0k13s\\_k](https://www.youtube.com/watch?v=0Fv-0k13s_k), Accessed 1/11/22, on behalf of QGEM Collaboration.
- [14] John S Bell, On the Einstein Podolsky Rosen paradox, *Phys. Phys. Fiz.* **1**, 195 (1964).
- [15] Nicolas Brunner, Daniel Cavalcanti, Stefano Pironio, Valerio Scarani, and Stephanie Wehner, Bell nonlocality, *Rev. Mod. Phys.* **86**, 419 (2014).
- [16] Charles H. Bennett et al, Mixed-state entanglement and quantum error correction, *Phys. Rev. A* **54**, 3824 (1996).
- [17] Ryan J. Marshman, Anupam Mazumdar, and Sougato Bose, Locality and entanglement in table-top testing of the quantum nature of linearized gravity, *Phys. Rev. A* **101**, 052110 (2020).
- [18] Suraj N. Gupta, Quantization of Einstein's gravitational field: Linear approximation, *Proc. Phys. Soc. London Sect. A* **65**, 161 (1952).
- [19] Suraj N. Gupta, Quantization of Einstein's gravitational field: General treatment, *Proc. Phys. Soc. London Sect. A* **65**, 608 (1952).
- [20] Daniel Carney, Philip C. E. Stamp, and Jacob M. Taylor, Tabletop experiments for quantum gravity: A user's manual, *Classical Quantum Gravity* **36**, 034001 (2019).
- [21] Marios Christodoulou, Andrea Di Biagio, Markus Aspelmeyer, Časlav Brukner, Carlo Rovelli, and Richard Howl, Locally mediated entanglement in linearized quantum gravity, *Phys. Rev. Lett.* **130**, 100202 (2023).
- [22] Marios Christodoulou and Carlo Rovelli, On the possibility of laboratory evidence for quantum superposition of geometries, *Phys. Lett. B* **792**, 64 (2019).
- [23] Alessio Belenchia, Robert M. Wald, Flaminia Giacomini, Esteban Castro-Ruiz, Časlav Brukner, and Markus Aspelmeyer, Quantum superposition of massive objects and the quantization of gravity, *Phys. Rev. D* **98**, 126009 (2018).
- [24] Daine L. Danielson, Gautam Satishchandran, and Robert M. Wald, Gravitationally mediated entanglement: Newtonian field versus gravitons, *Phys. Rev. D* **105**, 086001 (2022).
- [25] M. D. Scadron, *Advanced Quantum Theory* (World Scientific Publishing Company, Singapore, 2007).
- [26] Eric Poisson and Clifford M. Will, The gravitational self-force, in *General Relativity and Gravitation* (World Scientific, Singapore, 2005), pp. 119–141.
- [27] Paul Busch, Teiko Heinonen, and Pekka Lahti, Heisenberg's uncertainty principle, *Phys. Rep.* **452**, 155 (2007).
- [28] Charles W. Misner, Kip S. Thorne, and John Archibald Wheeler, *Gravitation* (Macmillan, London, 1973).
- [29] Luc Blanchet, Gravitational radiation from post-Newtonian sources and inspiralling compact binaries, *Living Rev. Relativity* **17**, 2 (2014).
- [30] Fabian Gunnink, Anupam Mazumdar, Martine Schut, and Marko Toroš, Gravitational decoherence by the apparatus in the quantum-gravity-induced entanglement of masses, *Classical Quantum Gravity* **40**, 235006 (2023).
- [31] Ulrich K. Beckering Vinckers, Álvaro de la Cruz-Dombriz, and Anupam Mazumdar, Smearing out contact terms in ghost-free infinite derivative quantum gravity, [arXiv:2402.18694](https://arxiv.org/abs/2402.18694).
- [32] Sumanta Chakraborty, Anupam Mazumdar, and Ritapriya Pradhan, Distinguishing Jordan and Einstein frames in gravity through entanglement, *Phys. Rev. D* **108**, L121505 (2023).
- [33] Vijay Balasubramanian, Michael B. McDermott, and Mark Van Raamsdonk, Momentum-space entanglement and renormalization in quantum field theory, *Phys. Rev. D* **86**, 045014 (2012).
- [34] Christopher C. Gerry and Peter L. Knight, *Introductory Quantum Optics* (Cambridge University Press, Cambridge, England, 2023).
- [35] Ulf Leonhardt, *Essential Quantum Optics: From Quantum Measurements to Black Holes* (Cambridge University Press, Cambridge, England, 2010).
- [36] Marko Toroš, Anupam Mazumdar, and Sougato Bose, Loss of coherence and coherence protection from a graviton bath, *Phys. Rev. D* **109**, 084050 (2024).

- [37] Eric Poisson, Adam Pound, and Ian Vega, The motion of point particles in curved spacetime, *Living Rev. Relativity* **14**, 1 (2011).
- [38] Michael A. Nielsen and Isaac L. Chuang, *Quantum Computation and Quantum Information* (Cambridge University Press, Cambridge, England, 2010).
- [39] Koenraad Audenaert, Jens Eisert, Martin B. Plenio, and Reinhard F. Werner, Entanglement properties of the harmonic chain, *Phys. Rev. A* **66**, 042327 (2002).
- [40] Gerardo Adesso, Alessio Serafini, and Fabrizio Illuminati, Extremal entanglement and mixedness in continuous variable systems, *Phys. Rev. A* **70**, 022318 (2004).
- [41] Alessio Serafini, Gerardo Adesso, and Fabrizio Illuminati, Unitarily localizable entanglement of Gaussian states, *Phys. Rev. A* **71**, 032349 (2005).
- [42] Christian Weedbrook, Stefano Pirandola, Raúl García-Patrón, Nicolas J. Cerf, Timothy C. Ralph, Jeffrey H. Shapiro, and Seth Lloyd, Gaussian quantum information, *Rev. Mod. Phys.* **84**, 621 (2012).
- [43] Samuel L. Braunstein and Peter van Loock, Quantum information with continuous variables, *Rev. Mod. Phys.* **77**, 513 (2005).
- [44] N Canosa, Swapan Mandal, and R Rossignoli, Exact dynamics and squeezing in two harmonic modes coupled through angular momentum, *J. Phys. B* **48**, 165501 (2015).